Acta Chemica Scandinavica A 33 (1979) 719–725

Pyrite Like Phases in the Rh—Se System

ARNE KJEKSHUS,[a] TROND RAKKE[a] and ARNE F. ANDRESEN[b]

[a] Kjemisk Institutt, Universitetet i Oslo, Blindern, Oslo 3, Norway and [b] Institutt for Atomenergi, N-2007 Kjeller, Norway

The phase and structural relations in the Rh–Se system (from 66 to 74 atomic % Se; between 400 and 1100 °C) have been studied by X-ray and neutron diffraction, density, metallographic, and DTA measurements. $Rh_{1-t}Se_2$ (max. comp. range $0.02 \leqq t \leqq 0.24$) takes the pyrite type structure with disordered distribution of Rh atoms and vacancies. Rh_3Se_8 is strictly stoichiometric and in its pyrite like structure Rh atoms and vacancies are ordered.

Among the binary TX_2 compounds (T=transition metal, X=main group V or VI element) with one or more of the related structure types FeS_2-p (p=pyrite),[1-3] FeS_2-m (m=marcasite),[4,5] $CoSb_2$ (ternary prototype FeAsS – arsenopyrite),[6] α-$NiAs_2$ (pararammelsbergite),[7-9] $PdSe_2$,[10] $IrSe_2$,[11] and Rh_3Se_8 ($Rh_{0.75}Se_2$),[12] those for which T=Rh or Ir and X=S, Se, or Te appear to deserve more careful attention. As demonstrated by the brief summary in Table 1 of recorded Rh and Ir chalcogenides with ≧66 atomic % X there is a pattern in the phase and structural relationships for these phases. More detailed explorations are, *inter alia*, expected to elucidate the factors that govern the relative stability of the structure types FeS_2-p, $IrSe_2$, Rh_3Se_8, and also $Cd(OH)_2$.

The authors have earlier obtained a relatively detailed view of the Rh–Te system between 66 and 74 atomic % Te, and 400 and 1100 °C.[13] In the present paper we report the results of a similar study on the Rh–Se system, which despite considerable previous attention[12,14-21] still needs further development.

EXPERIMENTAL

Samples were prepared [from 99.999 % Rh powder (Johnson, Matthey & Co.) and 99.998 % Se (Bolidens Gruvaktiebolag)] and characterized according to essentially the same procedure as was used in the earlier study of the rhodium tellurides.[13] The experimental details concerning quenching experiments, metallographic examinations, X-ray and neutron diffraction, density, and DTA measure-

Table 1. Rh–X and Ir–X phases with 66 to 74 atomic % X according to Ref. 13.

X	Rh		Ir	
S	–		IrS_2	: $IrSe_2$ type.
	Rh_3S_8	: FeS_2-p like, a new variety?	Ir_3S_8	: FeS_2-p like, ordered and disordered?
Se	$RhSe_2$	: $IrSe_2$ type.	$IrSe_2$	: Prototype.
	$Rh_{1-t}Se_2$	: FeS_2-p type, homog. range.	–	
	Rh_3Se_8	: Prototype.	Ir_3Se_8	: FeS_2-p like, ordered and disordered?
Te	$Rh_{1+u}Te_2$	: $Cd(OH)_2$ type, homog. range.[a]	$IrTe_2$	: α[unknown type] $\rightleftarrows$ β[$Cd(OH)_2$ type].
	$Rh_{1-t}Te_2$	: FeS_2-p type, homog. range.	–	
	Rh_3Te_8	: Rh_3Se_8 type.	Ir_3Te_8	: FeS_2-p like, ordered and disordered?

[a] Stops at 65.5 atomic % Te.

0302-4377/79/100719-07$02.50

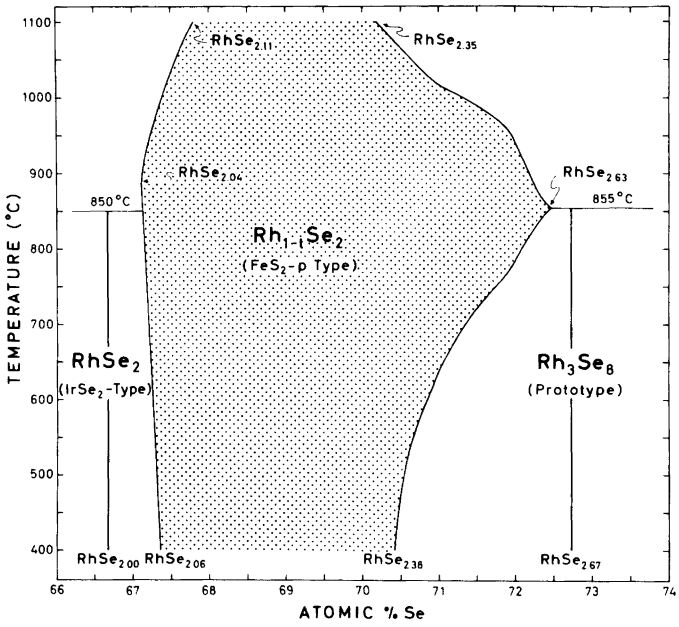

Fig. 1. Section of Rh–Se phase diagram.

ments, as well as the data processing, were also performed as referred in Ref. 13. 0.584×10^{-12} and 0.780×10^{-12} cm were taken as the nuclear scattering lengths of Rh and Se, respectively.[22]

PHASE ANALYSIS

A phase diagram has been published for the Rh–Se system,[20] making this and the Rh–Te[13] system special among the Rh–*X* and Ir–*X* systems. However, our preliminary results showed that the Rh–Se phase diagram needed some revision over the entire ranges of composition and temperature.

The Rh–Se system matches that of Rh–Te[13] in complexity, but despite marked similarities there are also distinct differences. Several of the (at least 22) phases with <66 atomic % Se involve rather time-consuming preparations and/or particular cooling or quenching treatments in order to be obtained in the pure state. Since, moreover the latter compositional range falls outside the present scope, the attention will here be focused on the range above 66 atomic % Se.

Within the range 66 to 74 atomic % Se there exist three intermediate phases in the Rh–Se system (Table 1). A revised section of the Rh–Se phase diagram from 66 to 74 atomic % Se and between 400 and 1100 °C is shown in Fig. 1, the basic data being produced according to the same experimental procedure as was used to explore the corresponding portion of the Rh–Te phase diagram.[13] From our comprehensive set of basic data we have only selected the unit cell dimension *a versus* the compositional parameter *t* relationship for quenched $Rh_{1-t}Se_2$ samples shown in Fig. 2.

The orthorhombic $RhSe_2$ phase exhibits a narrow homogeneity range. Its decomposition at 850±6 °C is somewhat sluggish and usually undetected by DTA. Between 720 and 850 °C, the composition of the phase appears to be $RhSe_{1.97}$.* A homogeneity range is found between 500 and 720 °C (at 500 °C: $RhSe_{1.98}$ to $RhSe_2$). Equilibrium is attained very slowly below 500 °C, but here the homogeneity range becomes very narrow and may be centered around $RhSe_2$. Further work on this phase is in progress.

The homogeneity range of the cubic $Rh_{1-t}Se_2$ phase varies with temperature (Fig. 1) and at about 890 °C the Rh richest composition, $Rh_{0.98}Se_2$, is found. The most Se rich composition corresponds

* Gross formulae or atomic % Te are used to denote nominal compositions.

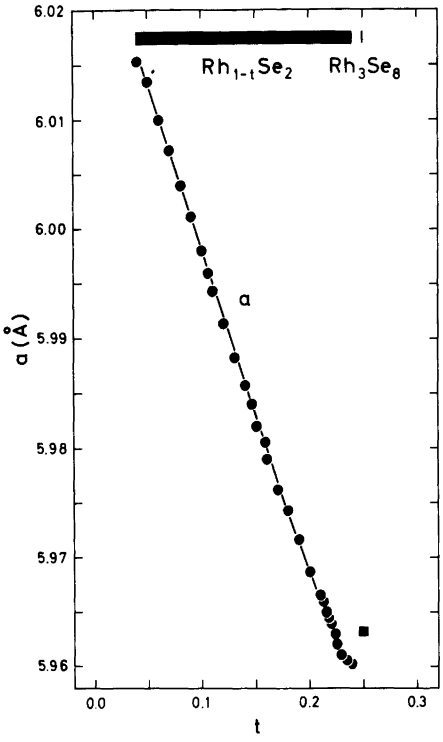

Fig. 2. Unit cell dimension of $Rh_{1-t}Se_2$ as function of compositional parameter t. Samples quenched from 850 to 900 °C. Data for Rh_3Se_8 are included for comparison. (Probable errors do not exceed size of symbols.)

to $Rh_{0.76}Se_2$ at 855±4 °C, which is also the temperature where the rhombohedral, stoichiometric Rh_3Se_8 phase undergoes peritectic decomposition: $Rh_{0.75}Se_2(s) \rightarrow Rh_{0.76}Se_2(s) +$ "Se(l)" (not DTA detectable).

At temperatures above 200 °C, no intermediate phase appears to exist between 74 and 100 atomic % Se. No solid solubility of Rh in Se could be detected for samples quenched or slowly cooled from 200 °C. (The samples were first treated at higher temperatures, slowly cooled to 200 °C, and then annealed at this temperature for about one year.) If an eutectic is formed between Rh_3Se_8 and Se, it must be located very close to Se.

STRUCTURES

The structural properties of the $Rh_{1-t}Se_2$ phase match those of $Rh_{1-t}Te_2$.[13] The observed densities

Table 2. Unit cell dimensions (from Guinier photographic data) and positional parameters (from neutron diffraction data) for $Rh_{1-t}Se_2$ at 22 °C. Standard deviations are given in parentheses. (Space group $Pa3$; (1-t)Rh in 4(a), Se in 8(c); final reliability factors ranging between 0.016 and 0.019.)

	$Rh_{0.98}Se_2$	$Rh_{0.90}Se_2$	$Rh_{0.85}Se_2$	$Rh_{0.78}Se_2$
a(Å)	6.0153(6)	5.9981(5)	5.9820(7)	5.9639(6)
x	0.3800(4)	0.3826(5)	0.3827(5)	0.3829(4)

(ranging between 7.87 g/cm³ for $Rh_{0.98}Se_2$ and 7.43 g/cm³ for $Rh_{0.78}Se_2$) show that the unit cell contains four $Rh_{1-t}Se_2$ formula units. The atomic arrangement is of the FeS_2-p type, with Rh atoms and vanacies (denoted □ in the formulae) distributed at random in the metal sub-lattice. The unit cell dimensions and positional parameters for the samples studied by neutron diffraction are given in Table 2. The defect concentrations (t) were independently confirmed by varying the occupation number parameter in preliminary profile refinement cycles.

The variations with t of the bonding interatomic distances and angles in $Rh_{1-t}Se_2$ are shown in Fig. 3. This illustration reveals the same features as were found for $Rh_{1-t}Te_2$.[13]

Rh_3Se_8 crystallizes rhombohedrally with one Rh_3Se_8 formula unit per unit cell (density 7.32 g/cm³). The structure is a distorted variant of the FeS_2-p type with an ordered distribution of Rh atoms and vacancies ($Rh_{3/4}\square_{1/4}Se_2$).[12] No indications of any disordering of the Rh atoms and vacancies could be observed by X-ray diffraction examination of quenched samples or in the high temperature X-ray diagrams of Rh_3Se_8. The variation of the unit cell dimensions of Rh_3Se_8 with temperature is shown in Fig. 4.

The profile refinement of the present neutron diffraction data for Rh_3Se_8 confirms that the findings of Hohnke and Parthé[12] are essentially correct. Comparison of the cell dimensions and positional parameters listed in Table 3 with those of Hohnke and Parthé show small discrepancies, the only clearly significant one being found for y_{II}. However, the effect of these small changes on the bonding interatomic distances and angles (Table 3 and Fig. 3) is more prominent. The results for Rh_3Se_8 and Rh_3Te_8[13] now comply, and it is in particular worth noting that the $Se_I - Se_I$ bond length indeed differs from that of $Se_{II} - Se_{II}$. Refer-

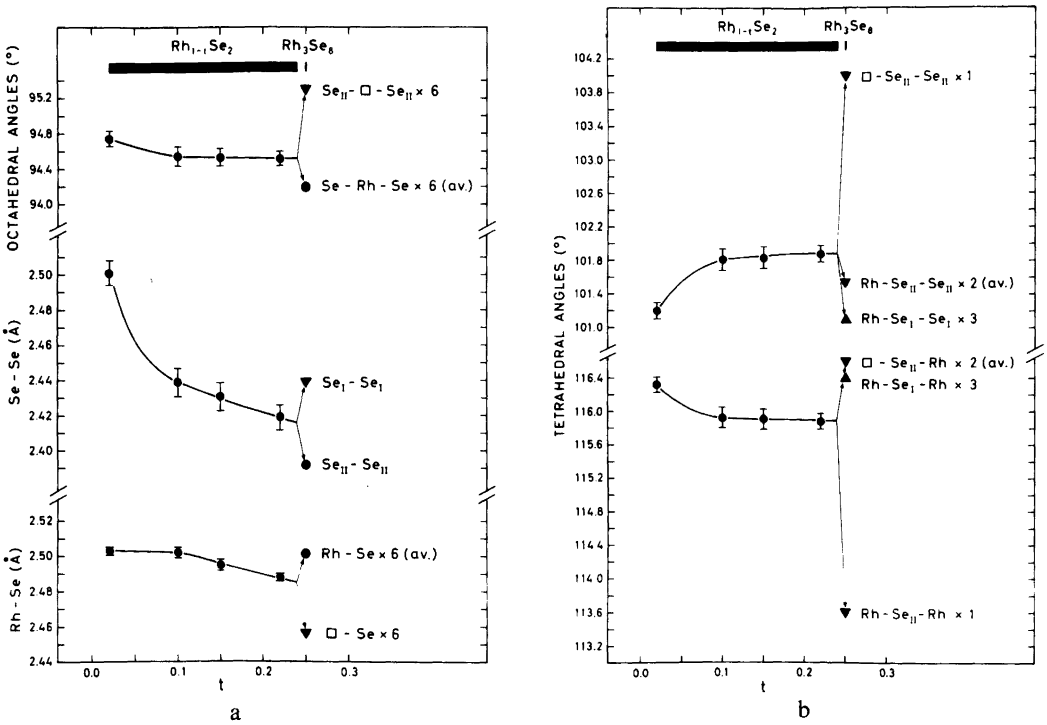

Fig. 3. Variation of bond lengths (a) and bond angles (b) for $Rh_{1-t}Se_2$ with t, and in relation to Rh_3Se_8.

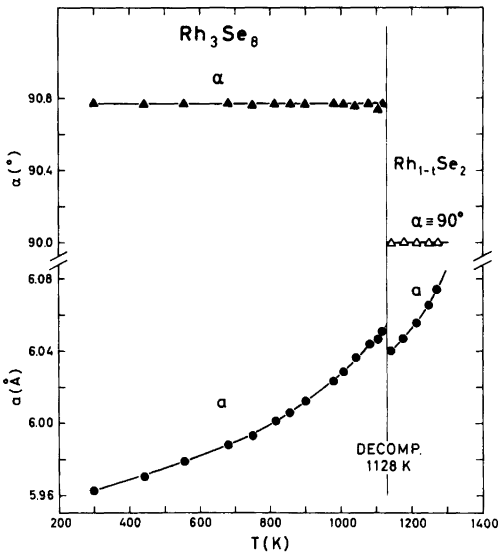

Fig. 4. Unit cell dimensions of (rhombohedral) Rh_3Se_8 *versus* temperature. Above 1128 K: $Rh_3Se_8 \rightarrow Rh_{1-t}Se_2$ with variable t. (Probable errors do not exceed size of symbols.)

ence is made to Refs. 12 and 13 for illustrations, descriptions, and comments concerning the Rh_3Se_8 type structure.

BONDING CONSIDERATIONS

A customary and convenient zeroth approach to the bonding situation in compounds with FeS_2-*p* type structure is to take an ionic ($T^{2+}X_2^{2-}$) starting point (*cf.*, *e.g.*, Refs. 23–28). The purely ionic picture is then modified by charge transfer from X_2^{2-} to T^{2+}, which besides reducing the effective ionic charges also contributes to broadening of the energy levels into bands.

The internal bonding within the $X-X$ pair is considered to be of the localized covalent nature and involves one bonding (σ_{X-X}) and one antibonding (σ_{X-X}^*) energy level. This is baked into all schemes from the very beginning and is maintained essentially unaffected by the further developments. Six orbitals per $X-X$ pair are accordingly available for bond formation with a corresponding number of T orbitals. The covalent platform, as its ionic precursor, attributes X character to the bonding

Table 3. Structural data for Rh_3Se_8 at 22 °C. [Unit cell dimensions (Guinier technique), and positional parameters (neutron diffraction technique); standard deviations in parentheses; space group $R\bar{3}$: Rh in 3(*e*) Se_I in 2(*c*), Se_{II} in 6(*f*); final reliability factor 0.018. Distances in Å and angles in degrees.]

a	5.9632(4)	Rh – Se_I × 2	2.497(4)
α	90.774(8)	Rh – Se_{II} × 2	2.506(3)
x_I	0.3803(7)	Rh – Se_{II} × 2	2.499(3)
x_{II}	0.8886(5)	□ – Se_{II} × 6	2.456(3)
y_{II}	0.1138(5)	Se_I – Se_I × 1	2.439(12)
z_{II}	0.6206(5)	Se_{II} – Se_{II} × 1	2.392(8)
Se_I – Rh – Se_{II} × 2	86.7(1)	Rh – Se_I – Rh × 3	116.4(2)
Se_I – Rh – Se_{II} × 2	93.3(1)	Rh – Se_I – Se_I × 3	101.1(2)
Se_I – Rh – Se_{II} × 2	83.8(1)	Rh – Se_{II} – Rh × 1	113.6(1)
Se_I – Rh – Se_{II} × 2	96.2(1)	□ – Se_{II} – Rh × 1	115.4(1)
Se_{II} – Rh – Se_{II} × 2	86.9(1)	□ – Se_{II} – Rh × 1	117.8(1)
Se_{II} – Rh – Se_{II} × 2	93.1(1)	Rh – Se_{II} – Se_{II} × 1	101.7(1)
Se_{II} – □ – Se_{II} × 6	84.7(1)	Rh – Se_{II} – Se_{II} × 1	101.4(1)
Se_{II} – □ – Se_{II} × 6	95.3(1)	□ – Se_{II} – Se_{II} × 1	104.0(1)

$T-X$ orbitals, whereas the anti-bonding $T-X$ orbitals inherit more from T. According to the current jargon the bonding and anti-bonding $T-X$ interactions give rise to σ_{T-X} and σ_{T-X}* energy bands, respectively.

At all stages of the model development, the octet rule or the parallel, generalized (8 – N) rule is a handly tool for the assignment of an overall valence state for T (v_T).[29] At first sight, phases which exhibit ranges of homogeneity appear to represent a complication in this connection because of the implied variation in v_T. Here the FeS_2-*p* type/like rhodium chalcogenides seem attractive as test cases.

Following this scheme $v_{Rh} = 2$ for $t = 0$ in $Rh_{1-t}X_2$. Thus, an overall d^7 manifold should be associated with T (*viz.* an essentially non-bonding d^6 and the additional electron in a σ_{T-X}* band). For increasing t, v_{Rh} should increase and become 3 for $t = 1/3$ (implying that the electrons contained in σ_{T-X}* are gradually drained off, down to empty at $t = 1/3$). The metallic, superconducting properties reported[30] for $Rh_{1-t}Se_2$ and $Rh_{1-t}Te_2$ are consistent with this picture. Semiconductivity and diamagnetism are to be expected for $t = 1/3$, and such properties are, in fact, assigned[19] to RhX_3 (and IrX_3) with postulated metal deficient FeS_2-*p* type structures. However, the latter assignments are clearly inconsistent with the present knowledge (*vide supra* and Ref. 13), and the most likely explanation is that the diamagnetic, semiconducting properties rather belong to Rh_3X_8 (and Ir_3X_8). The assumed errors in the composition assignments would be easily understandable, but the problem is now to account for the properties of T_3X_8.

According to the above recipe $v_T = 8/3$ for T_3X_8. The natural inference is then that one electron per T_3X_8 unit is accommodated in a σ_{T-X}* band, which in turn would suggest that T_3X_8 should be metallic. However, maintaining that T_3X_8 is semiconducting there appear to be two simple possibilities, *viz.* either that the electron pair bond concept is valid and the generalized (8 – N) rule framework open for rejection, or the other way round. We like to plead that the second alternative provides the basis for a consistent explanation of the results for $Rh_{1-t}X_2$ and Rh_3X_8. σ_{X-X} is here no longer ascribed pure X character, but is assumed to also carry a degree of $T-X$ character. In other words, the electrons involved in the $X-X$ bonds have no longer well defined identity, but mingle to some extent with those belonging to the $T-X$ pool. (According to the ionic formalism the modified approach can be contemplated as a mixture of $T^{2+}X_2{}^{2-}$ and $T^{4+}2X^{2-}$.)

The above attitude reflects essential features of the valence bond theory, and it is therefore only natural to consider adoption of other concepts from this field. Pauling[31] has, *e.g.*, formulated two frequently used relations between bond length (l) and bond number (n). Neglecting various correction terms, both these relations follow

$$l_n = l_1 - f \log n \qquad (1)$$

Pauling distinguishes only between cases with fractional ($n<1$ with $f=0.60$) and multiple bonds ($n>1$ with $f=0.71$). However, it seems unreasonable that f should be constant within such large classes of compounds and phases. Even for the closely related elements within a given group of the Periodic System some variation is to be expected. The larger sized atoms with the more diffuse electron clouds are, *e.g.*, likely to permit a larger variation in l for a given change in n than the smaller atoms prior to them in the group. To correct for this deficiency we propose that f itself varies logarithmically according to

$$f = k \log (1 + l_1) \qquad (2)$$

where k is a constant for the elements of a given group of the Periodic System.

In order to try the thus modified relation on the results for $Rh_{1-t}X_2$ and Rh_3X_8 we have chosen the reference data from the FeS_2-*p* type compounds $MgO_2[l_1(O)=1.49$ Å$]$,[32] $MnS_2[l_1(S)=2.03$ Å$]$,[33] $MnSe_2[l_1(Se)=2.33$ Å$]$,[33] and $MnTe_2[l_1(Te)=2.74$ Å$]$,[33] which appear to exhibit clear-cut bonding situations. Introducing $l_2(O)=1.21$ Å[34] from the O_2 molecule $k=2.35$ is obtained. The derived values for f are 0.93, 1.13, 1.23, and 1.35 for O, S, Se, and Te, respectively. The O–O bond length of 1.35 Å[35] in NaO_2 gives $n=1.43$ which is close enough to the expected value of 1.5 to provide a reasonable check of consistency. Furthermore, for the S_2, Se_2, and Te_2 molecules,[34] values of $n=1.33$, 1.30, and 1.25, respectively, are obtained as apparently realistic measures for the decreasing double bond character.

Returning to the $Rh_{1-t}X_2$ and Rh_3X_8 phases, $2n$ (calculated according to eqns. 1 and 2) can be interpreted as the effective number of electrons involved in the $X-X$ bond. The corresponding valences are then

$$v_{Rh} = 2(2-n)/(1-t) \qquad (3)$$

for $Rh_{1-t}X_2$, and

$$v_{Rh}' = 2(2-n_I)/3 + 2(2-n_{II}) \qquad (4)$$

for Rh_3X_8, where n_I and n_{II} refer to the X_I-X_I and $X_{II}-X_{II}$ bonds, respectively. The variations of v_{Rh} and $2n$ with the compositional parameter t are illustrated in Fig. 5. The shapes and levels of the curves in Fig. 5 look promising from the model point of view. The fact that v_{Rh} becomes very nearly 3 at $t=0.25$ certainly inspires confidence, since this would be consistent with an emptied σ_{T-X}^* band (*vide supra*) and hence with the inferred semiconducting properties of Rh_3X_8.

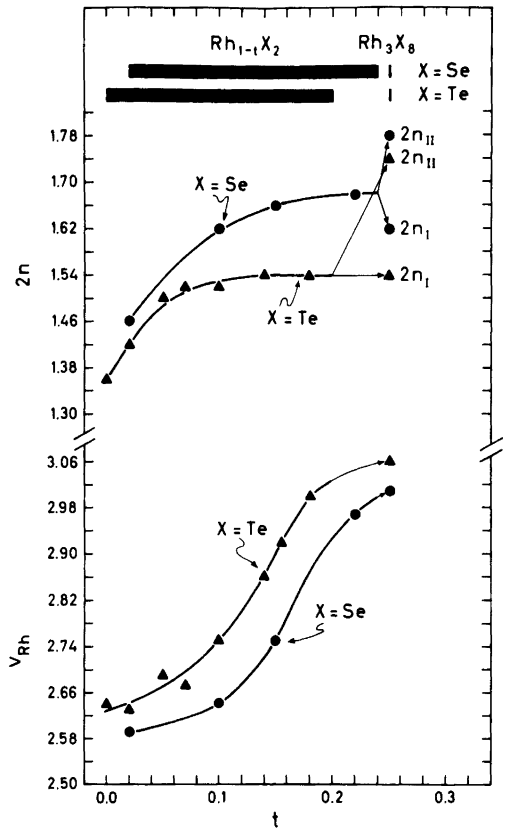

Fig. 5. Rh valence (v_{Rh}) and effective number of electrons in $X-X$ bonding ($2n$) *versus* t for $Rh_{1-t}X_2$ and Rh_3X_8. (v_{Rh} and $2n$ calculated according to eqns. 1–4.)

Acknowledgement. This work has received financial support from The Norwegian Research Council for Science and the Humanities.

REFERENCES

1. Bragg, W. L. *Proc. R. Soc. London A 89* (1914) 468.
2. Ewald, P. P. and Friedrich, W. *Ann. Phys. Paris 44* (1914) 1183.

3. Brostigen, G. and Kjekshus, A. *Acta Chem. Scand. 23* (1969) 2186.
4. Buerger, M. J. *Am. Mineral. 16* (1931) 361.
5. Brostigen, G., Kjekshus, A. and Rømming, C. *Acta Chem. Scand. 27* (1973) 2791.
6. Zhdanov, G. S. and Kuz'min, R. N. *Soviet Phys. Crystallogr. 6* (1962) 704.
7. Stassen, W. N. and Heyding, R. D. *Can. J. Chem. 46* (1968) 2159.
8. Fleet, M. E. *Am. Mineral. 57* (1972) 1.
9. Kjekshus, A. and Rakke, T. *To be published.*
10. Grønvold, F. and Røst, E. *Acta Crystallogr. 10* (1957) 329.
11. Barricelli, L. B. *Acta Crystallogr. 11* (1958) 75.
12. Hohnke, D. and Parthé, E. *Z. Kristallogr. 127* (1968) 164.
13. Kjekshus, A., Rakke, T. and Andresen, A. F. *Acta Chem. Scand. A 32* (1978) 209.
14. Wöhler, L., Ewald, K. and Krall, H. G. *Ber. Dtsch. Chem. Ges. 66* (1933) 1638.
15. Biltz, W. *Z. Anorg. Allg. Chem. 233* (1937) 282.
16. Geller, S. and Cetlin, B. B. *Acta Crystallogr. 8* (1955) 272.
17. Steen, Ø. *Thesis*, University of Oslo, Norway 1955.
18. Haraldsen, H. *Experientia Suppl. 7* (1957) 165.
19. Hulliger, F. *Nature (London) 204* (1964) 644.
20. Rummery, T. E. and Heyding, R. D. *Can. J. Chem. 45* (1967) 131.
21. Parthé, E., Hohnke, D. and Hulliger, F. *Acta Crystallogr. 23* (1967) 832.
22. *The 1976-compilation of the Neutron Diffraction Commission.*
23. Haraldsen, H. *Avhandl. Norske Videnskaps-Akad. Oslo I, Mat. Naturv. Kl.* (1947) No. 4.
24. Hulliger, F. and Mooser, E. *Prog. Solid State Chem. 2* (1965) 330.
25. Hulliger, F. and Mooser, E. *J. Phys. Chem. Solids 26* (1965) 429.
26. Brostigen, G. and Kjekshus, A. *Acta Chem. Scand. 24* (1970) 2993.
27. Goodenough, J. B. *J. Solid State Chem. 3* (1971) 26.
28. Goodenough, J. B. *J. Solid State Chem. 5* (1972) 144.
29. Kjekshus, A. and Rakke, T. *Struct. Bonding (Berlin) 19* (1974) 45.
30. Matthias, B. T., Corenzwit, E. and Miller, C. E. *Phys. Rev. 93* (1954) 1415.
31. Pauling, L. *The Nature of the Chemical Bond*, Cornell University Press, Ithaca 1960.
32. Kjekshus, A. and Rakke, T. *To be published.*
33. Hastings, J. M., Elliott, N. and Corliss, L. M. *Phys. Rev. 115* (1959) 13.
34. Wells, A. F. *Structural Inorganic Chemistry*, Oxford University Press, Oxford 1967.
35. Ziegler, M., Rosenfeld, M., Känzig, W. and Fischer, P. *Helv. Phys. Acta 49* (1976) 57.

Received April 17, 1979.